

FDTD/TDPO HYBRID APPROACH FOR ANALYSIS OF THE EM SCATTERING OF COMBINATIVE OBJECTS

L.-X. Yang, D.-B. Ge, and B. Wei

School of Science
Xidian University
Xi'an 710071, China

Abstract—A time-domain hybrid approach that combines the Finite-Difference Time-Domain (FDTD) method with Time Domain Physical Optics (TDPO) is presented. The approach can be applied to the analysis of the backscattering of combinative objects including a Small-Size structure (SS) and a Large-Size structure (LS) with respect to the wavelength of interest. When dealing with the coupling of SS to LS, the near-to-near field extrapolation technique based on Kirchhoff's surface integral representation is used and a sequential transfer method is developed. According to the time domain calculation sequence in FDTD, the contribution of SS to LS is transferred directly to far zone observation point. The sequential transfer method has some advantages in high efficiency and small amounts of computer memory. For far zone back scattering, the influence of LS onto SS can be obtained by using the reciprocity theorem. Finally, the validation and application examples are presented, demonstrating the accuracy and effectiveness of this approach.

1. INTRODUCTION

The development of high power microwave antenna, aviation and space techniques has motivated the interest in electromagnetic scattering problems involving combinative objects. The combinative objects are composed by two separate parts: one is a Small-Size (SS) structure and the other is a Large-Size (LS) part with respect to the wavelength of interest, such as line-surface structure objects, a reflector antenna and a satellite with large wingspan. Generally, neither rigorous numerical schemes nor asymptotic techniques is easily be implemented in evaluating the time domain scattering or wideband RCS for combinative objects accurately and efficiently. Therefore

the hybrid algorithm combining numerical scheme with asymptotic technique is invoked in dealing with this class of problems.

Several hybrid formulations have been reported. However, most of them implement the numerical method or asymptotic technique in frequency domain [1–3]. To analyze time domain phenomena the transform from frequency domain to time domain via an inverse Fourier Transform is necessary, that however results in a decreased physical insight into the overall process. Time domain analysis has become particularly important due to its superiority in the straightforward analysis of transient phenomena and its ability to obtain a wideband response in frequency domain in once computation. The development of a hybrid scheme with all its steps realized in time domain is of interest. Such a hybrid scheme combining the Finite-Difference Time-Domain (FDTD) method [4] with Time Domain Physical Optics [5] (TDPO) is considered and the radiation of a monopole antenna mounted on a large but finite size PEC plate is determined in [6]. The FDTD and TDPO are applied to treat two separate parts, monopole and plate, respectively, in this problem. The coupling between them is not however considered in this example because the monopole is an ideal forced excitation source.

In this paper, a time-domain hybrid approach that combines FDTD method with TDPO is presented for the scattering problem by combinative objects, in which the coupling must be considered by any means. The FDTD and TDPO are taken to treat the SS structure and LS part, separately. To compute the coupling field between SS and LS parts, the scattering by single part, either LS or SS, is evaluated firstly and the scattered field from one part is considered as the illuminating wave for the other one. In order to receive higher efficiency and need less memory storage in computation, we furthermore develop a sequential transfer algorithm, in which the coupling contributions from one to the other part are transferred directly to the far zone observation point according to the marching-on in time sequence.

2. PRINCIPLE OF THE HYBRID APPROACH

Considering the configuration of combinative objects, the computation domain is firstly split into FDTD region and TDPO region, enclosing the SS structure and LS part, respectively. The far field $\mathbf{e}(\mathbf{r}, t)$ can be divided into four terms as follows:

$$\mathbf{e}(\mathbf{r}, t) = \mathbf{e}^S(\mathbf{r}, t) + \mathbf{e}^L(\mathbf{r}, t) + \mathbf{e}^{SL}(\mathbf{r}, t) + \mathbf{e}^{LS}(\mathbf{r}, t) \quad (1)$$

The first term \mathbf{e}^S represents the far field directly scattering by the SS structure. It can be easily calculated from FDTD with a near-

to-far field transformation. The second term e^L represents the far field directly scattering by LS part. It can be determined thanks to the TDPO expressions. The last two terms in Eq. (1) represent the secondary scattered field due to the coupling between FDTD and TDPO region. To obtain the coupling field between two regions, the scattered field from one region is considered as the illuminating wave onto the other region.

2.1. Finite Difference Time Domain (FDTD)

The Finite Difference Time Domain method has been demonstrated to be an accurate and efficient method to simulate the interaction of electromagnetic waves with all kinds of obstacles, including the target of complex material and complex configuration [7, 8]. This method is formulated by discrete Maxwell's curl equation over a finite volume and the derivatives with centered difference approximation in both time and space. Due to the finite capabilities of computers used to implement the finite difference equations, the mesh must be limited in the three directions. Typically, the discretization step is used to being chosen lower $\lambda_{\min}/10$, where λ_{\min} is the smallest wavelength. For simulations where the modeled region must extend to infinity, absorbing boundary conditions (ABCs) are employed at the outer lattice truncation planes. When calculating the far zone fields, near-to-far-field transformation is employed [9, 10]. There is no need to extend the FDTD space lattice to the far field. Therefore, this technique requires prohibitive computational time and memory space when the studied structures are large compared to the wavelength.

2.2. Time Domain Physical Optics (TDPO)

Physical optics is a high frequency approximation technique. It is assumed that the surface current on illuminated side of a body is determined only by the incident wave, whereas over the shadowed portion the surface current is equal to zero. TDPO is the time domain version of PO. For a perfectly conducting body, the far scattering field in time-domain as follows [5]:

$$\begin{aligned} \mathbf{E}^s(\mathbf{r}, t) &= (Z_0/4\pi rc) \times \iint_{s'} \hat{\mathbf{r}} \times \left[\hat{\mathbf{r}} \times \frac{\partial}{\partial t} \mathbf{J}_s(\mathbf{r}', t - \tau) \right] ds' \\ \mathbf{H}^s(\mathbf{r}, t) &= -(1/4\pi rc) \times \iint_{s'} \hat{\mathbf{r}} \times \frac{\partial}{\partial t} \mathbf{J}_s(\mathbf{r}', t - \tau) ds' \end{aligned} \quad (2)$$

Where τ is the time retardation. Surface-current density distribution \mathbf{J}_s is written as

$$\mathbf{J}_s(\mathbf{r}', t) = \begin{cases} 2\hat{\mathbf{n}}' \times \mathbf{h}^{inc}(\mathbf{r}', t) & \text{in the lit region} \\ 0 & \text{otherwise} \end{cases} \quad (3)$$

Where \mathbf{h}^{inc} is the incident magnetic field. The scattered field can be determined by Eqs. (1) and (2) if the magnetic field incident on the scatterer is known.

2.3. Coupling between TDPO Region and FDTD Region

The dominant technique of the FDTD/TDPO hybrid approach then consists in the interaction between the two regions. First, we consider the influence of FDTD region onto TDPO region, as shown in Fig. 1, providing the primary scattered field by SS structure has been obtained by using FDTD method.

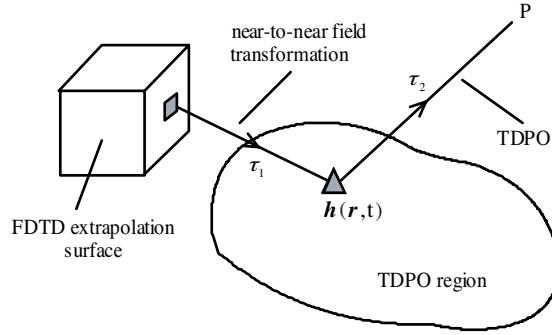


Figure 1. Principle of coupling FDTD region to TDPO region.

In order to find the illuminating field onto LS part in TDPO region from SS structure in FDTD region, the near-to-near field extrapolation technique in FDTD based on Kirchoff's surface integral representation [11] is invoked, because FDTD region is close to TDPO region. The field illuminated on the surface of LS part can then be expressed as

$$\mathbf{h}(\mathbf{r}, t + \tau) = \oint_s \left\{ -(\hat{\mathbf{n}}' \cdot (\mathbf{r} - \mathbf{r}')) \left[\frac{\mathbf{h}'(\mathbf{r}', t)}{4\pi|\mathbf{r} - \mathbf{r}'|^3} + \frac{\partial \mathbf{h}'(\mathbf{r}', t)}{\partial t} \right] - \frac{\partial \mathbf{h}'(\mathbf{r}', t)}{\partial n} \right\} ds' \quad (4)$$

At time step $n + 1$, the time and space derivatives in (4) are approximated by a second-order center difference. After some manipulations we may obtain

$$h(\mathbf{r}, n + 1 + \tau/\Delta t) = F_1(n) + F_2(n + 1) + F_3(n + 2) \quad (5)$$

Where F_1, F_2 and F_3 are sequences in different time steps, detailed expressions of them can be found in [11].

Let the LS surface in TDPO region be divided into M triangular patches, and the recorded time steps in calculation are $n\Delta t$ ($n = 1, 2, \dots, N$). In order to obtain the incident magnetic field for every time step and each allocation point on the surface, the memory storage requires at least $M \times N^+$, where $N^+ > N$. The continuance of the arrival waveform in time domain will last much longer than $N\Delta t$ because of retardation from SS to LS part.

To reduce the requirement of computer storage, a sequential transfer scheme is developed. In every time step, we perform FDTD extrapolation from a cell on FDTD output boundary to a patch on the surface of LS part, followed immediately by TDPO computation of contribution from this patch to the far field observation point. These data are then stored and summed up to form the scattered waveform in time domain according to the retardation between a cell-to-patch and a patch-to-observation point, respectively. This treatment proceeds until the marching-on in time procedure is over. The flowchart of sequential transfer scheme is depicted in Fig. 2.

The Substitution of (5) into the expressions (2) and (3) gives

$$\begin{aligned} \mathbf{E}(\mathbf{r}, n + 1 + (\tau_1 + \tau_2)/\Delta t) = & \\ & A \iint_{s'} \hat{\mathbf{r}} \times \left\{ \hat{\mathbf{r}} \times \left[\hat{\mathbf{n}} \times \hat{\mathbf{x}} \left[\dot{F}_1(n) + \dot{F}_2(n + 1) + \dot{F}_3(n + 2) \right]_{hx} \right] \right\} ds' \\ & + A \iint_{s'} \hat{\mathbf{r}} \times \left\{ \hat{\mathbf{r}} \times \left[\hat{\mathbf{n}} \times \hat{\mathbf{y}} \left[\dot{F}_1(n) + \dot{F}_2(n + 1) + \dot{F}_3(n + 2) \right]_{hy} \right] \right\} ds' \\ & + A \iint_{s'} \hat{\mathbf{r}} \times \left\{ \hat{\mathbf{r}} \times \left[\hat{\mathbf{n}} \times \hat{\mathbf{z}} \left[\dot{F}_1(n) + \dot{F}_2(n + 1) + \dot{F}_3(n + 2) \right]_{hz} \right] \right\} ds' \quad (6) \end{aligned}$$

Where $A = Z_0/(2\pi rc)$, $\dot{F}_i = \partial F_i/\partial t$. It is observed that there are F terms with different time steps in the right of (6). In order to obtain the $\mathbf{E}(n^*)$ in observation point, storing the value at the last time step is necessary, and additional memory is required.

Here, a different strategy is used. We note that \mathbf{E} is a sequence in discrete time, where $n^* = \text{int} \{n + 1 + (\tau_1 + \tau_2)/\Delta t\}$. At the $(n + 1)$ th time step, $F_1(n + 1), F_2(n + 1)$ and $F_3(n + 1)$ are calculated, and only

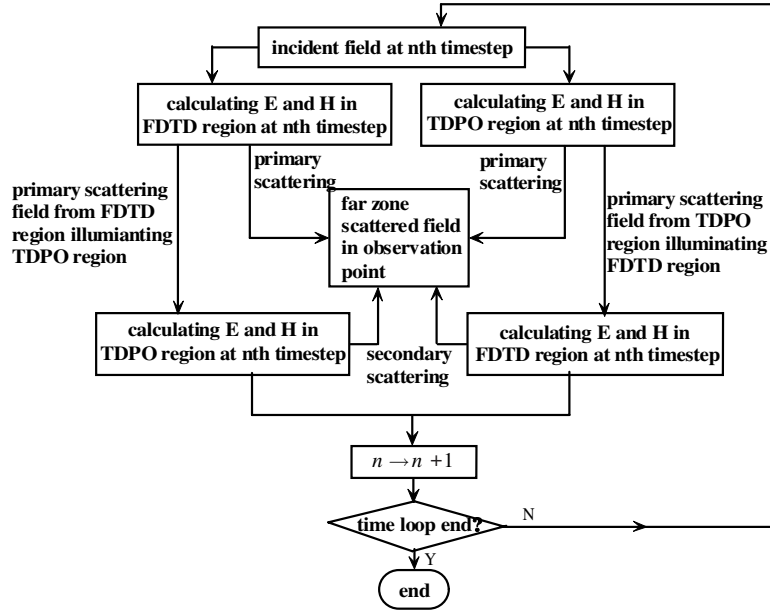


Figure 2. Flowchart of sequential transfer scheme.

$F_2(n+1)$ contributes to $\mathbf{E}(n^*)$. $F_1(n+1)$ and $F_3(n+1)$ are added to registers $\mathbf{E}(n^*+1)$ and $\mathbf{E}(n^*-1)$ in a consistent manner respectively. This scheme is explained in the diagram shown in Fig. 3, where the arrows indicate the contribution to the \mathbf{E} sequence from the FDTD and TDPO iterations.

In other words, the contribution from the field on FDTD output boundary at $n+1$ time step is respectively added to the register (n^*+1) , n^* and (n^*-1) with corresponding coefficients. This procedure is repeated for each subsurface. This treatment proceeds until the marching-on in time procedure is over. It is evident that the LS part in TDPO region is only a transfer stage, and no additional computer memory is required.

In principle, the first-order scattering field by LS part in TDPO region is considered as the illuminating field on the LS structure in FDTD region, when analyzing the coupling of TDPO to FDTD region. The illuminating wave from LS part to SS structure can be introduced through the connection boundary in FDTD region. However, it can be deduced based on the reciprocity theorem [12] that the secondary scattering fields produced by FDTD region are identical to the one by TDPO region in co-polarized backscattering case that simplifies the computation.

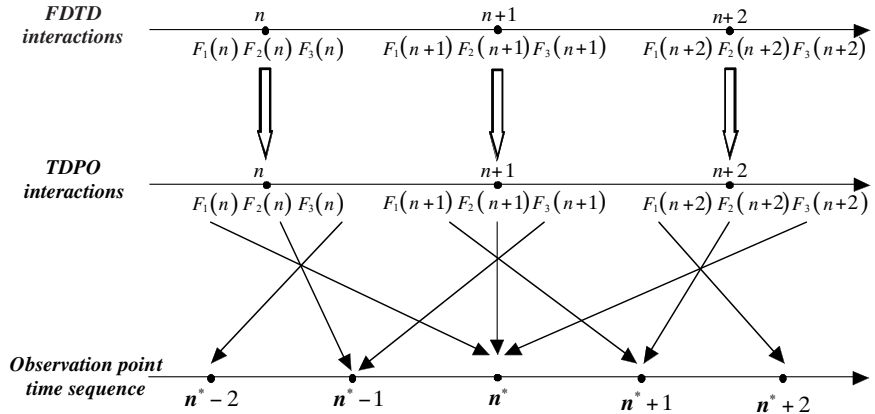


Figure 3. Diagram showing how the terms constituting the surface integral contribute to $\mathbf{E}(n^*)$.

3. NUMERICAL RESULTS

As the first example, we consider the radiation characteristics of a dipole nearby a PEC plate of finite size. The dipole is placed at a distance of 0.41 m over the center of a plate of dimension $1.8 \times 1.5 \text{ m}^2$ and is excited by Gaussian pulse

$$p(t) = 10^{-10} \exp \left[- \left(\frac{t - 3T}{T} \right)^2 \right] \quad T = 1 \text{ ns} \quad (7)$$

A calculation based on the hybrid method has been performed (circle line in Fig. 4), where the dipole represents the FDTD region and the whole surface of the plate represents the TDPO region. For comparison, FDTD result (solid line) is also depicted in the same figure, where the dipole and plate are enclosed in the computed domain. The two results are mainly in agreement. Some discrepancies still exist in the later time, because the TDPO is an asymptotic technique, and the diffraction at edges is neglected, but FDTD is a full-wave method.

Next we consider an example of the backscattering by combinative objects composed by a PEC cube and plate, as shown in Fig. 5. A modulated Gaussian pulse with frequency ranging from 200 MHz to 300 MHz, and pulse width 30 ns excites the combinative objects. The incident wave travels in the xoz plane with $\theta = 45^\circ$ with its electric field parallel to the y -axis. The backscattering for co-polarization is to be determined. First, we consider the primary scattering coming from the PEC cube set as an SS structure, and plate as the LS part, respectively.

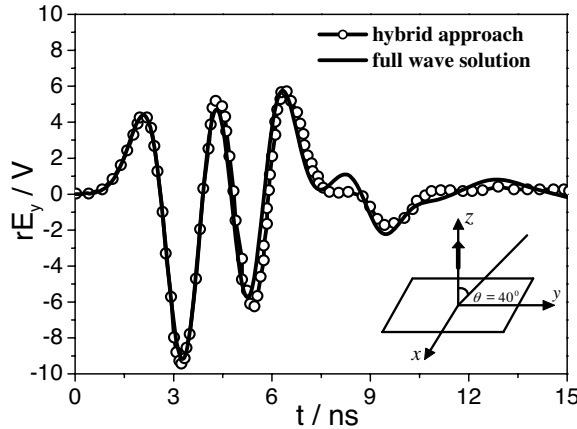


Figure 4. The far zone field in time domain.



Figure 5. Combinative object composed by cube and plate.

To calculate the primary scattering, we set FDTD region containing the cube, and TDPO region enclosing the plate. The backscattering for co-polarization is depicted in Fig. 6, in which the circles represent the summation of two primary scattered fields. To compute the secondary scattering, we apply the sequential transfer algorithm described in previous section to calculate the coupling of FDTD to TDPO region. This computation procedure is, in fact, performed with the marching on in time procedure in FDTD computation. The total scattered field by the combinative cube and plate is denoted by solid line in Fig. 6. It is observed that the two results with and without the coupling secondary scattering coincide in early time and the discrepancies appear in later time. This is reasonable because of the retardation of secondary scattering with respect to the primary scattering.

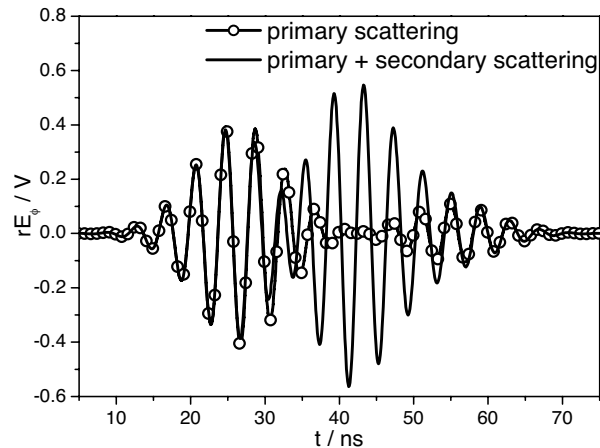


Figure 6. Backscattered waveform in time domain for co-polarization.

4. CONCLUSION

A time-domain hybrid approach that combines the FDTD with TDPO is presented. The approach can be applied to the analysis of the electromagnetic backscattering by combinative objects including both SS and LS. The scattered fields are partitioned into primary and secondary scattering. The primary scattering is treated by FDTD and TDPO, respectively. For evaluating the coupling field, a sequential transfer method is developed. The coupling contribution is transferred directly to far zone observation point from one part via the other one according to the marching-on in time sequence. This algorithm needs small amounts of computer memory and achieves high efficiency.

ACKNOWLEDGMENT

This work is supported by the National Defense Foundation of China and the Graduate Innovation Fund, Xidian University (No.05023).

REFERENCES

1. Nie, X.-C., Y.-B. Gan, N. Yuan, C.-F. Wang, and L.-W. Li, "An efficient hybrid method for analysis of slot arrays enclosed by a large radome," *J. of Electromagn. Wave and Appl.*, Vol. 20, No. 2, 249–264, 2006.

2. Jakobus, U. and M. L. Friedrich, "Improved PO-MM hybrid formulation for scattering from three-dimensional perfectly conducting bodies of arbitrary shape," *IEEE Trans. on Antennas and Propagat.*, Vol. 43, No. 2, 162–169, 1995.
3. Wang, Y., K. C. Sujeet, and S. N. Safieddin, "An FDTD/ray-tracing analysis method for wave penetration through inhomogeneous walls," *IEEE Trans. On Antennas and Propagat.*, Vol. 50, No. 11, 1598–1604, 2002.
4. Taflove, A., *Computational Electrodynamics: The Finite-Difference Time-Domain Method*, Artech House, Norwood, MA, 1995.
5. Sun, E.-Y. and W. V. T. Rusch, "Time-domain physical-optics," *IEEE Trans. On Antennas and Propagat.*, Vol. 42, No. 1, 9–15, 1994.
6. Le Bolzer, F., R. Gillard, J. Citerne, V. Fouad Hanna, and M. F. Wong, "An hybrid formulation combining FDTD and TDPO," *1998 IEEE Int. Antennas Propagat. Symp. Dig.*, Vol. 2, No. 36, 952–955, 1998.
7. Gong, Z. Q. and G. Q. Zhu, "FDTD analysis of an anisotropically coated missile," *Progress In Electromagnetics Research*, PIER 64, 69–80, 2006.
8. Qian, Z. H., R. S. Chen, K. W. Leung, and H. W. Yang, "FDTD analysis of microstrip patch antenna covered by plasma sheath," *Progress In Electromagnetics Research*, PIER 52, 173–183, 2005.
9. Ayestar, R. G. and F. Las-Heras, "Near field to far field transformation using neural networks and source reconstruction," *J. of Electromagn. Wave and Appl.*, Vol. 20, No. 15, 2201–2213, 2006.
10. Ferrara, F., C. Gennarelli, R. Guerriero, G. Riccio, and C. Savarese, "An efficient near-field to far-field transformation using the planar wide-mesh scanning," *J. of Electromagn. Wave and Appl.*, Vol. 21, No. 3, 341–357, 2007.
11. Ramahi, O. M., "Near- and far-field calculations in FDTD simulations using Kirchhoff surface integral representation," *IEEE Trans. on Antennas and Propagat.*, Vol. 45, No. 5, 753–759, 1997.
12. Guo, L.-X., Y.-H. Wang, and Z.-S. Wu, "Application of the equivalence principle and the reciprocity theorem to electromagnetic scattering from two adjacent spherical objects," *Acta Physica Sinica*, Vol. 55, No. 11, 5815–5823, 2006 (in Chinese).